RSC Applied Polymers

ROYAL SOCIETY OF CHEMISTRY

PAPER

View Article Online
View Journal | View Issue

Cite this: *RSC Appl. Polym.*, 2024, **2**, 205

Facile fabrication of a stretchable, stable, and self-adhesive poly(ionic liquid) as a flexible sensor†

Jingxian Sun, [b] Shilu Zhou,[b] Zhe Zhao,[b] Fengfeng Zhang,[b] Zhongcheng Guo,[b] Shimin Liu[b] and Yan Lu*[a]

Received 10th August 2023,
Accepted 2nd December 2023

DOI: 10.1039/d3lp00137g

rsc.li/rscapplpolym

Although poly(ionic liquid)s (PILs) are alternative materials to flexible hydrogel sensors owing to their unique characteristics such as nonvolatility, high conductivity, and excellent temperature tolerance, their weak mechanical properties greatly limit their application in flexible sensors. In this study, a PIL with high stretchability, excellent stability, and remarkable self-adhesive property was fabricated by the *in situ* photopolymerization of 1-vinyl-3-butylimidazolium bis(trifluoromethylsulfonylimide) ([VBIM]TFSI) and butyl acrylate (BA) in 1-butyl-3-methylimidazolium bis(trifluoromethylsulfonylimide) ([BMIM]TFSI). The outstanding electromechanical properties, including instant response, improved stretchability, low hysteresis, and prominent repeatability, of the resulting PIL imparted it with strain-sensing capacity for recognizing a variety of physical deformations, such as human joint activity and pulse. Moreover, since the change in the conductivity of PILs with temperature conforms to the Vogel–Tamman–Fulcher (VTF) equation, the PIL could be utilized as a high-performance temperature sensor. Thus, this work provides a facile strategy for fabricating a high-performance bimodal PIL sensor, which has broad prospects for flexible electronics.

1. Introduction

As an essential component of next-generation electronics, flexible sensors, especially strain sensors, which are used to convert external changes into electrical signals, have attracted increasing attention for their wide range of applications in flexible electronics, including wearable electronics, human-interactive systems, artificial skins, and robots.[1–4] As typical flexible sensors, nanocomposite-based flexible sensors are generally prepared by integrating conductive nanofillers (such as graphene, carbon nanotubes, and metal nanowires) in elastomeric polymer matrixes, which usually exhibit high sensitivity to monitor small deformations,[5–8] but poor stretchability and obvious hysteresis, which is caused by the modulus mismatch between the soft matrix and the solid conductive network.[9,10] Recently, in order to avoid the abovementioned defects of nanocomposite strain sensors, ionic conductors have been developed as flexible sensors due to their unique features, such as high conductivity, superior stretchability, and excellent transparency.[11–13] As representative ionic conductors, ionic conductive hydrogels have been extensively investigated.[14] However, they usually suffer from environmental instability, including easy drying and easy freezing, which greatly limits their applications.[15,16]

Ionic liquids (ILs) are organic salts consisting of organic cations and inorganic/organic anions, which normally have melting points below 100 °C.[17,18] Ionic liquids possess unique characteristics, such as high ionic conductivity, ultralow volatility, excellent temperature resistance, low flammability, tunable polarity, and controllable basicity/acidity.[19,20] They are alternative materials to address the environmental instability of hydrogels. Recently, some researchers encapsulated ionic liquids in polymers to form conductive channels to obtain strain sensors with high stretchability and low hysteresis.[21–23] However, these sensors may suffer from ionic liquid leaks. Directly polymerizing ionic liquids to obtain poly(ionic liquid)s is an effective approach to solve this problem.[24–26] PILs have both the characteristics of ionic liquids and the flexibility of polymers, which enables them to be applied in various electronics field, especially electrolytes.[27–30] Nevertheless, owing to their limited mechanical properties, PILs usually cannot satisfy the demands for flexible sensors. Although some researchers tried to improve the mechanical properties of PILs, there are only a few reports of PILs with high mechanical properties, and the most common approach is to adjust the structure of ionic liquids to form intermolecular interactions in ionic liquids, such as hydrogen bonds, electrostatic interactions, and ionic dipole interactions.[31,32] For example, Sun *et al.* synthesized a mechanically strong polymerized zwitterion gel by utilizing the dipole–dipole interactions between mole-

[a]*State Key Laboratory of Solid Lubrication, Lanzhou Institute of Chemical Physics, Chinese Academy of Sciences, Lanzhou 730000, China. E-mail: luyan@licp.cas.cn*
[b]*China Tobacco Shandong Industrial Co. Ltd, Jinan 250000, P. R. China*
† Electronic supplementary information (ESI) available. See DOI: https://doi.org/10.1039/d3lp00137g

cules.[33] However, these methods depend on the molecular structure of ionic liquids and are not universal. If the ionic liquids cannot form specific intermolecular interactions between molecules, the formed PILs usually have poor mechanical properties. For instance, because of their hydrophobicity, ionic liquids containing bis(trifluoromethylsulfonylimide) anions ($TFSI^-$) have been widely used, but there are only a few related reports of PILs composed of $TFSI^-$ with high mechanical properties.

In this work, by *in situ* photopolymerizing [VBIM]TFSI and BA in ionic liquid [BMIM]TFSI, a PIL with excellent mechanical properties was obtained. Moreover, the fabricated PIL exhibited superior stability and desirable self-adhesion. Benefiting from its remarkable electromechanical performances, including high stretchability, instant response, exceptional sensitivity, prominent durability, and low electrical hysteresis, the PIL could be utilized as a flexible strain sensor to detect a variety of human activities, such as joint movement and pulse. In addition, the conductivity change of the PIL with temperature conforms to the VTF equation, which indicated the potential of the PIL to serve as a temperature sensor with high response speed, sensitivity, as well as repeatability. Therefore, the synthesized PIL with enhanced mechanical properties is an ideal candidate for flexible electronics.

2. Experimental section

Materials

Butyl acrylate (BA) and acrylic acid (AA) were ordered from Energy Chemical. 1-Vinyl-3-butylimidazolium bis(trifluoromethylsulfonylimide) ([VBIM]TFSI), 1-butyl-3-methylimidazolium bis(trifluoromethylsulfonylimide) ([BMIM]TFSI), and 1-ethyl-3-methylimidazolium chloride ([EMIM]Cl) were purchased from Meryer Chemical. 1,6-Bis(acryloyloxy)hexane (HDDA), poly(ethylene glycol) diacrylate (PEGDA) and 2-hydroxy-2 methylpropiophenone (HMPP) (photoinitiator 1173) were purchased from Shanghai Aladdin Biochemical Technology Co., Ltd.

Methods

The PIL was synthesized *via* one-pot photopolymerization, applying [VBIM]TFSI and BA as the reactive monomers, [BMIM]TFSI as the ionic liquid, 1173 reagent as the photoinitiator, and HDDA as the crosslinker. Briefly, [VBIM]TFSI, BA, [BMIM]TFSI, photoinitiator 1173 and HDDA were blended in a certain ratio to generate a homogeneous solution. All the ratios of the reactants were relative to the content of reactive monomers. Then, the obtained solution was transferred into a silicone mold covered by glass sheets, which was followed by UV irradiation for 300 s with the intensity of 80 mW cm^{-2} at 365 nm to produce PIL. The PAA ionogel was synthesized by a similar approach, in which the *in situ* photopolymerization was conducted with AA as the monomer, [EMIM]Cl as the ionic liquid, 1173 reagent as the photoinitiator, and PEGDA as the crosslinker. The PAA hydrogel was fabricated by a similar method, applying AA as the monomers, water as the solution, 1173 reagent as the photoinitiator, and PEGDA as the crosslinker.

Characterization

The measurements of mechanical properties and adhesive strength were conducted on a digital tensile equipment (E44.104, MTS, China), in which the tensile rate was set on 100 mm min^{-1} and the lap shear testing method was utilized for the evaluation of adhesion. The complex impedance spectroscopy was recorded on an electrochemical workstation (CHI 604E, Chenhua Instrument, China). The conductivity of the sample was calculated by the equation $\sigma = L/(AR)$, where L is the thickness, A is the area, and R is the resistance. The transparency of the PIL was tested by a UV visible spectrophotometer (UV2310II, Tianmei, China) and the thickness of the sample was 1 mm. The thermal behavior was tracked by thermogravimetric analyses (TGA) (Q500, TA Instruments, New Castle, DE). The test was carried out at a scan rate of 10 °C min^{-1} under nitrogen atmosphere. The differential scanning calorimeter (DSC) (Q2000, TA Instruments, New Castle, DE) was applied to measure the glass transition temperature in nitrogen atmosphere. The characterization of the electromechanical performance and sensing performance was fulfilled with a combination of a universal testing instrument (E44.104, MTS, China) and a source meter (Keithley 2400).

3. Results and discussion

As illustrated in Scheme 1, the PIL was synthesized by polymerizing [VBIM]TFSI and BA in [BMIM]TFSI under UV irradiation with the introduction of HDDA as the cross-linker. Owing to the outstanding compatibility between the materials, a uniform, soft and transparent PIL without liquid leakage was obtained after irradiation. According to the literature,[34] unlike thermal polymerization, the photopolymerization features a very fast reaction rate. The preparation of the PIL could be completed in only tens of seconds. Therefore, this one-step synthesis is very facile and fast, which is beneficial for industrial production, as it endows the products with low cost and reliable quality.

For PILs, the weak mechanical properties are currently a major issue that hinders their application in flexible sensors. In this work, when BA was not added, the mechanical properties of the product formed by the polymerization of 70 wt% [VBIM]TFSI in 30 wt% [BMIM]TFSI were low, and the mechanical properties could not be measured by our tensile equipment. As demonstrated in Fig. 1a, with the addition of 5 wt% BA to the ionic liquids, the mechanical properties of the PIL were significantly improved. Both the tensile strength and stretchability of the PIL were improved with the increase of BA content. The copolymer molecular chain of the obtained PIL was composed of random soft BA segments and hard [VBIM]TFSI segments. The addition of BA reduced the rigidity of the polymer chain of the PIL, and a flexible and elastic material was thus formed. However, as illustrated in Fig. 1b, the

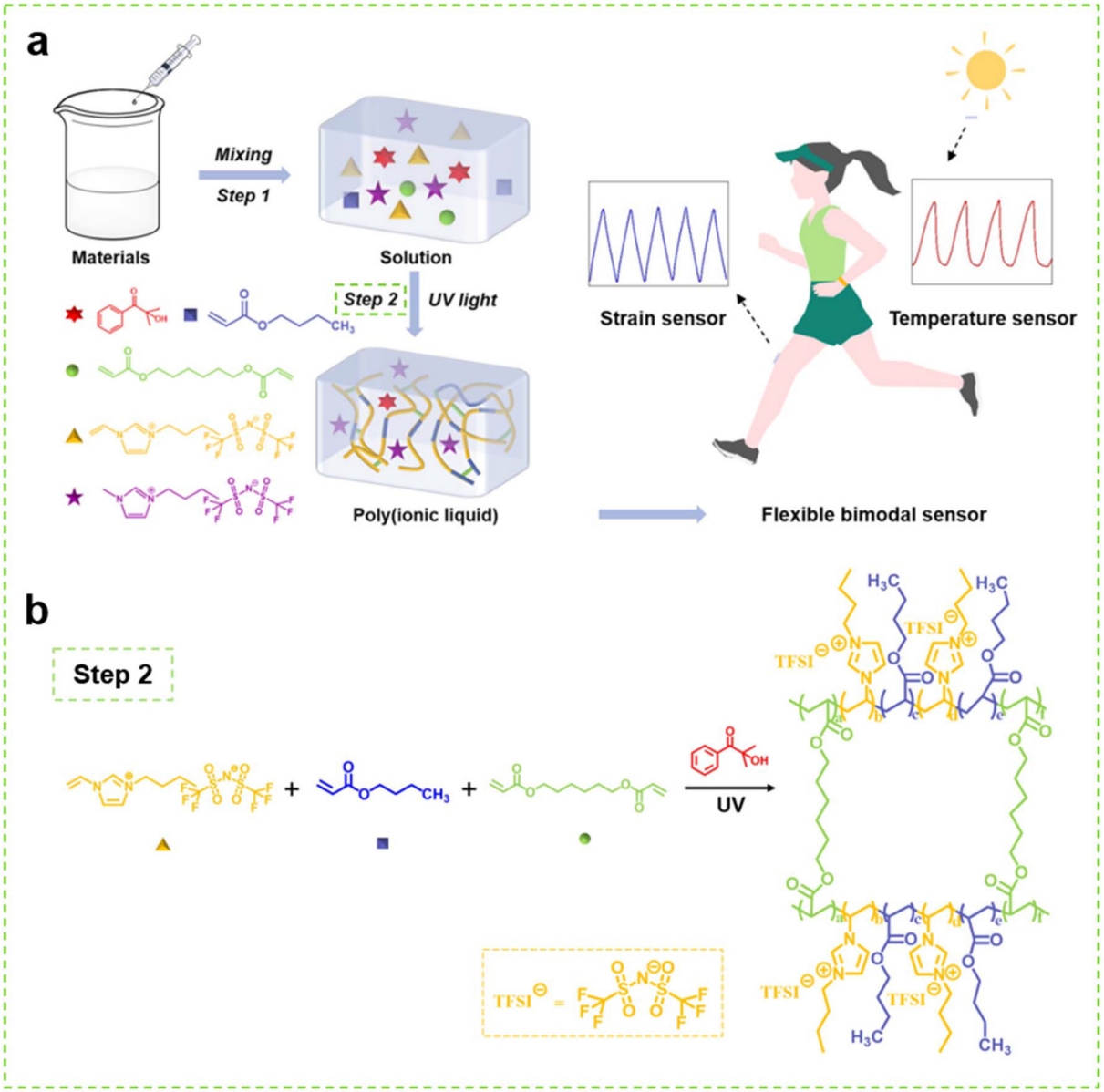

Scheme 1 (a) Schematic illustration of the preparation of the PIL and its application as flexible sensor, (b) Schematic illustration of the polymerization process of the PIL.

increase in the content of BA led to a decrease in the conductivity of the PIL. Hence, the content of BA was selected to be 10 wt%, which is enough to meet the requirements of mechanical properties for the utilization of PIL as a strain sensor. The chemical crosslinking agent can affect the characteristics of the PIL by adjusting the degree of crosslinking. According to the literature,[35,36] after the addition of bifunctional HDDA, the vinyl end of HDDA participated in the formation of the polymer backbone, so the dual vinyl ends of HDDA could connect two polymer backbone strands to bridge them. Therefore, as shown in Scheme 1b, HDDA could act as a crosslinker to make the molecular chains of the PIL form a network structure, which improves the mechanical properties of the PIL. As displayed in Fig. 1c and d, increasing the content of HDDA could improve the tensile strength of the PIL, but reduce the stretchability and the conductivity. Therefore, the content of HDDA was determined to be 0.4 wt% to ensure the PIL has suitable mechanical properties and conductivity. Ionic liquids are usually added to PILs to improve the conductivity of PILs. When a small amount of ionic liquid is added, some researchers still refer to the obtained material as PIL,[37,38] while some researchers call it an ionogel or PIL/IL.[31] In this work, a small amount of [BMIM]TFSI was added to the reaction system, and the resulting material was named PIL for simplicity. As shown in Fig. 1e and f, the mechanical properties of the PIL were enhanced by increasing the content of the [VBIM]

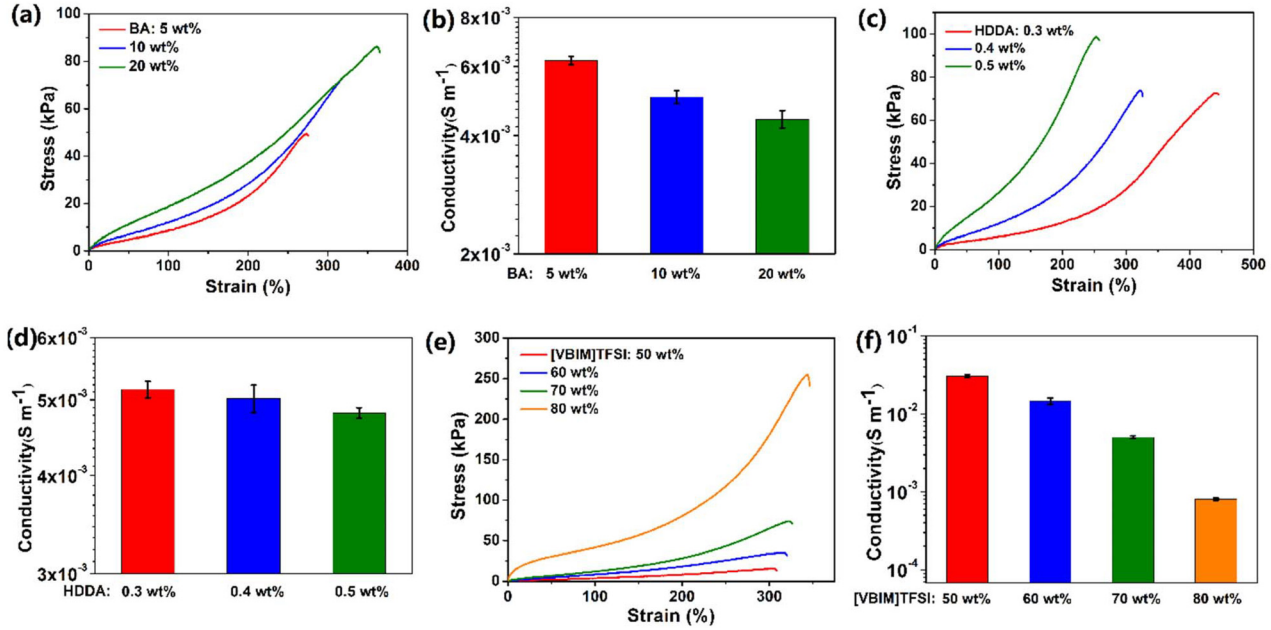

Fig. 1 (a) Tensile stress–strain results of the PIL with various BA concentrations. (b) Conductivities of the PIL with various BA concentrations. (c) Tensile stress–strain results of the PIL with various HDDA concentrations. (d) Conductivities of the PIL with various HDDA concentrations. (e) Tensile stress–strain tests of the PIL with various [VBIM]TFSI concentrations. (f) Conductivities of the PIL with various [VBIM]TFSI concentrations.

TFSI content, while the conductivity decreased. If the amount of non-polymerized ionic liquid in the system is too high, there is a risk of leakage of ionic liquid.[34] Therefore, in order to avoid the leakage of [BMIM]TFSI and balance the mechanical properties and conductivity of the PIL, the content of [VBIM]TFSI was finally determined to be 70 wt%. Finally, the solution was first mixed according to the mass ratio of [VBIM]TFSI to [BMIM]TFSI at 7 : 3, and then BA (10 wt% relative to the ionic liquids), photoinitiator 1173 (1 wt% relative to reactive monomers), and HDDA (0.4 wt% relative to reactive monomers) were added. The evenly mixed solution was illuminated by UV lamp, and a PIL with high mechanical properties and high conductivity was fabricated.

As shown in Fig. S1,† the obtained PIL has relatively good transparency (higher than 80% over the visible range), which is beneficial for electronics devices in which visible light is required in the inner parts. For hydrogel conductors, the low environmental stability greatly restricts their practical application, since the water of the hydrogels easily volatilizes at high temperature and freezes at low temperature. In contrast, the PIL exhibited excellent temperature resistance. The TGA curve in Fig. 2a demonstrates that the weight of the PIL did not change before 260 °C, indicating the superior thermal stability. It is worth noting that the TGA curve shows a continuous degradation process, which indicates that the degradation of the polymer and the volatilization of the free ionic liquid overlap (Fig. S2†). As depicted in the DSC data in Fig. 2b, the glass transition temperature of the PIL is about −60 °C, exhibiting its excellent low temperature resistance. In addition, the resulting polymer exhibited only one glass transition temperature, which proves that the raw materials are evenly mixed and there is no microphase separation in the obtained PIL. Although ionic liquids do not volatilize in the environment, our previous studies have shown that the ionogels containing hydrophilic ionic liquids are not stable.[39] In this work, to avoid this problem, hydrophobic ionic liquids were selected to prepare PIL. The PIL, PAA ionogel, and PAA hydrogel were prepared and maintained in an atmosphere at 15 °C and 30% RH to track their environmental stability. Fig. 2c demonstrates the rapid evaporation of water in the PAA hydrogel within the initial 12 h, indicating the poor environmental stability. In contrast, the PAA ionogel absorbed moisture from the air and eventually reached equilibrium. The final water absorption of the ionogels for entering equilibrium is connected with the humidity in the air, which benefits their application as humidity sensors, but hinders their stability as strain sensors.[39] The PIL composed of hydrophobic materials in this work was very stable with a weight loss of than 1%, displaying its admirable environmental stability, which greatly facilitates its practical application.

In recent decades, researchers have been pursuing the goal of endowing flexible sensors with self-adhesion to get rid of the inconvenience of using tape or cable ties. For ionic conductors, especially hydrogels, a common strategy to obtain self-adhesion is integrating dopamine into the matrix. However, this method also has some disadvantages, such as high price, complicated preparation, and poor repetitive adhesion. In this work, the PIL was synthesized with reference to pressure-sensitive adhesives to achieve self-adhesion. The ionic liquid [BMIM]TFSI could act as a plasticizer to reduce the Young's modulus of the PIL, endowing it with outstanding flexibility and fluidity. Thus, the intermolecular interactions

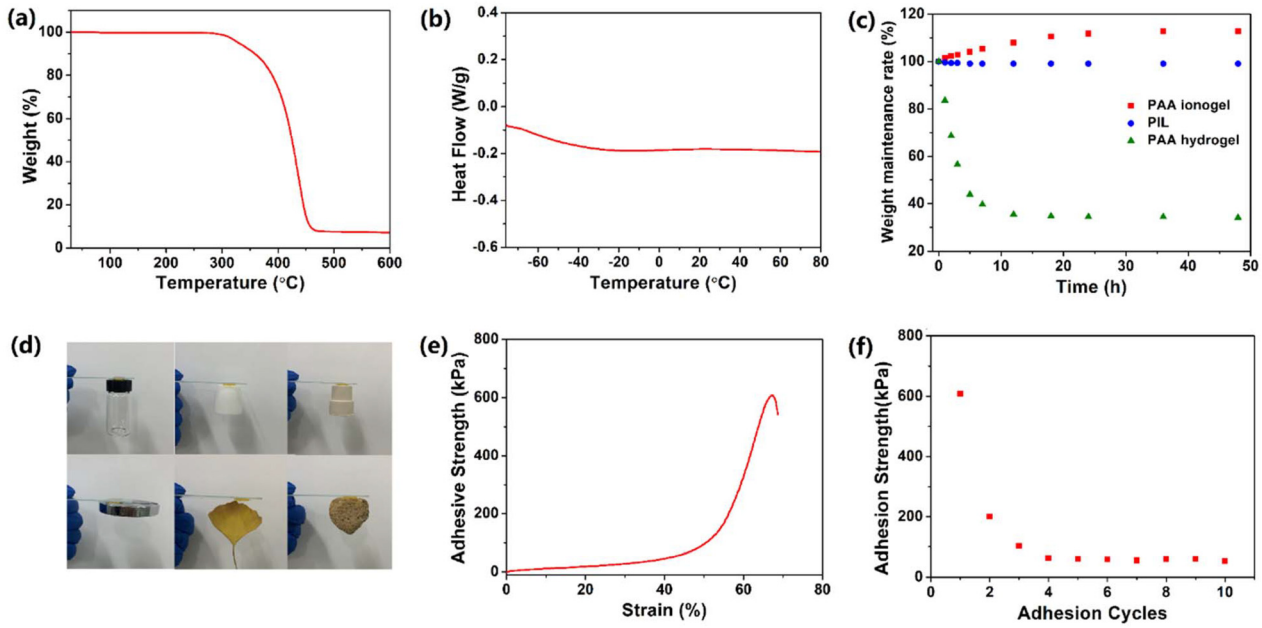

Fig. 2 (a) TGA curve of the PIL. (b) DSC curve of the PIL. (c) Weight change of the PAA ionogel, PIL and PAA hydrogel with time at 15 °C and 30% RH. (d) The PIL displays strong adhesion to diverse materials, including plastic, PTFE, rubber, steel, leaf and stone. (e) Tensile adhesion test curve of the PIL. (f) Repeatable adhesion characteristic of the PIL on a glass substrate.

can be ensured by the effective contact between the PIL and the substrate surface, including van der Waals forces, electrostatic interaction and hydrogen bonds, which contributes to the superior adhesion. As shown in Fig. 2d, the PIL could easily adhere to diverse materials, including plastic, PTFE, rubber metal, leaves, and stone. The adhesion strength of the PIL was characterized by the tensile shear experiment, in which the PIL was sandwiched in two glasses followed by a stretch with a digital tensile machine. The tensile shear curve is shown in Fig. 2e. In the first adhesion cycle, the adhesive force was mainly provided by the strong mechanical interlocking action. Therefore, the adhesion strength of the PIL could reach 600 kPa in the first adhesion cycle, which far exceeds most of the existing self-adhesive ionic conductors.[40–42] In addition to high adhesion strength, the PIL also possessed excellent repetitive self-adhesion. Due to the failure of the mechanical interlocking structure and the cohesive failure during the first tensile shear test, the adhesion strength of the PIL decreased to about 200 kPa in the second adhesion. However, the PIL still maintained about 60 kPa adhesion strength after several repetitions, indicating its outstanding repetitive self-adhesion. Therefore, the excellent self-adhesion of the PIL entitled it to sticking firmly on the surface of the object to improve the detection accuracy.

Benefiting from its remarkable flexibility, large stretchability and high conductivity, the PIL could be applied as a flexible strain sensor. For nanocomposite-based strain sensors, the resistance change mainly resulted from the destruction of a conductive network. However, for ionic conductors, the resistance change is derived from the change in its shape.[41] During the stretching process resulting from the decreases of the cross-sectional area, the resistance of the PIL enlarged. At small deformations, the resistance change of the PIL conforms to the following equation:

$$dR = \frac{\rho L_0}{A_0}\left(\frac{(1+2\upsilon)\varepsilon - \upsilon^2\varepsilon^2}{(1-\upsilon\varepsilon)^2}\right)$$

where dR is the resistance change of the PIL, ρ is the electrical resistivity of the PIL, A_0 is the cross sectional area of the unstretched PIL, ε is the applied strain, and ν is the Poisson's ratio of the PIL.[21,43] Therefore, the shape variable of the PIL can be calculated by detecting the change in its electrical signal, which is the working mechanism of the PIL as a strain sensor. As displayed in Fig. 3a, on applying a tensile force, the resistance of the PIL increased promptly. It reached equilibrium within about 200 ms, suggesting its exceptional response speed, which promotes the detection of instantaneous deformation. As shown in Fig. 3b, within about 50% strain, the resistance of the PIL changed linearly with the strain, and this good linear relationship facilitates the calibration and accuracy of the signal. However, with the increase of strain, the resistance change and the strain of the PIL cannot present good linearity, which is due to the inhomogeneous deformation of the PIL under large stretching. In Fig. 3c, an obvious change of the electrical signal is detected and stabilized under both small strain (1%, 5% and 10%) and large strain (20% and 100%), which indicates that the PIL possesses excellent detection capability in different strain ranges. Nanocomposite sensors usually have large hysteresis due to the incompatibility of the modulus of soft polymers and rigid

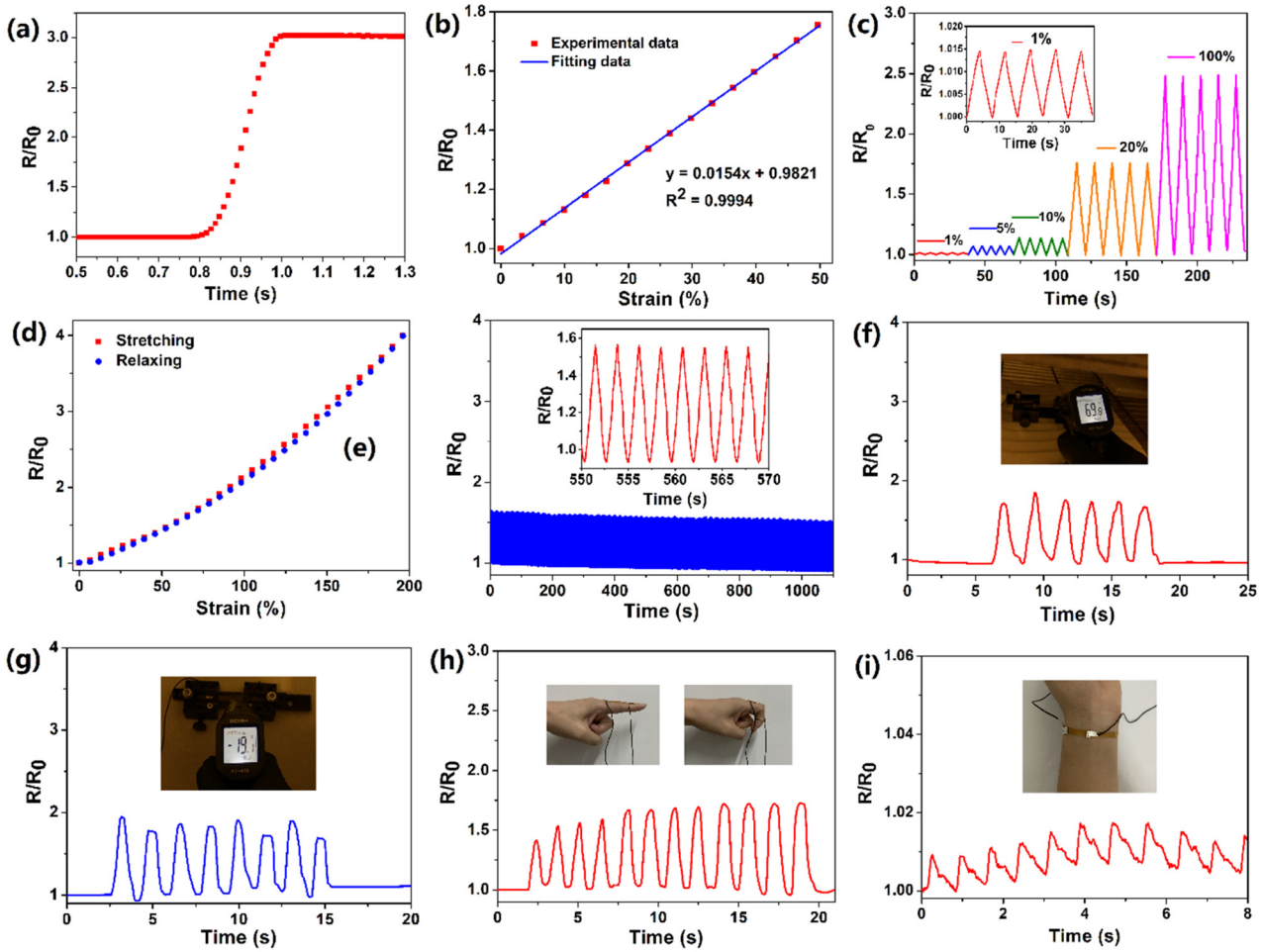

Fig. 3 (a) Response time of the PIL. (b) Resistance variation of the PIL as a function of strain. (c) Time-dependent resistance evolution of the PIL during 5 stretching–recovering cycles with different strains (1%, 5%, 10%, 20%, 100%). (d) Time-dependent resistance evolution of the PIL in a 200% stretching–relaxing cycle. (e) Time-dependent resistance evolution of the PIL with 50% strain over 500 cycles. (f) Time-dependent resistance evolution of the PIL at about 70 °C. (g) Time-dependent resistance evolution of the PIL at about −20 °C. (h) Time-dependent resistance evolution of the PIL for detecting the motion of a finger. (i) Time-dependent resistance evolution of the PIL for monitoring the human pulse.

fillers.[9] The degree of hysteresis (DH) is generally applied to represent the hysteresis, which follows the equation:

$$\mathrm{DH} = \frac{A_{\mathrm{loading}} - A_{\mathrm{unloading}}}{A_{\mathrm{loading}}} \times 100\%$$

where A_{loading} and $A_{\mathrm{unloading}}$ are the areas of the loading and unloading curves, respectively.[9] According to the calculation of the data in Fig. 3d, the DH of the PIL holds a value of about 1.54 at 200% strain, which was smaller than most values of the reported strain sensors,[10] exhibiting an extremely small hysteresis. The gauge factor (GF) is usually used to express the sensitivity of the strain sensors, which can be calculated by:

$$\mathrm{GF} = \frac{\Delta R/R_0}{\Delta L/L_0}$$

where R_0 and ΔR are the initial value and the value change of the resistance, respectively, and L_0 and ΔL are the initial value and the value change of the length, respectively.[39] The GF value of the PIL was calculated as about 2 at 200% strain, indicating higher sensitivity compared to other ionic conductor sensors.[9,10] As another important indicator of strain sensors, the durability and stability remain a major challenge for most strain sensors. For example, the easy dehydration of the hydrogel usually degenerated the performances of the strain sensors. As illustrated in Fig. 3e, during 500 stretching cycles, the electrical signal change curve of the PIL exhibited remarkable repeatability, indicating its superior stability and durability. For hydrogel ionic conductor sensors, the instability at high and low temperatures greatly restricts their application. Compared with hydrogels, PILs can be used at higher temperatures and lower temperatures. As demonstrated in Fig. 3f and g, benefiting from its exceptional temperature resistance, the PIL could maintain stable electromechanical properties at about 70 °C and −20 °C, demonstrating its wider working range than hydrogels. Many strain sensors still find it challenging to detect a wide range of mechanical deformations with only one sensor. For instance, nanocomposite strain sensors typically have high sensitivity toward detecting small deformations, but lack enough stretchability to detect large

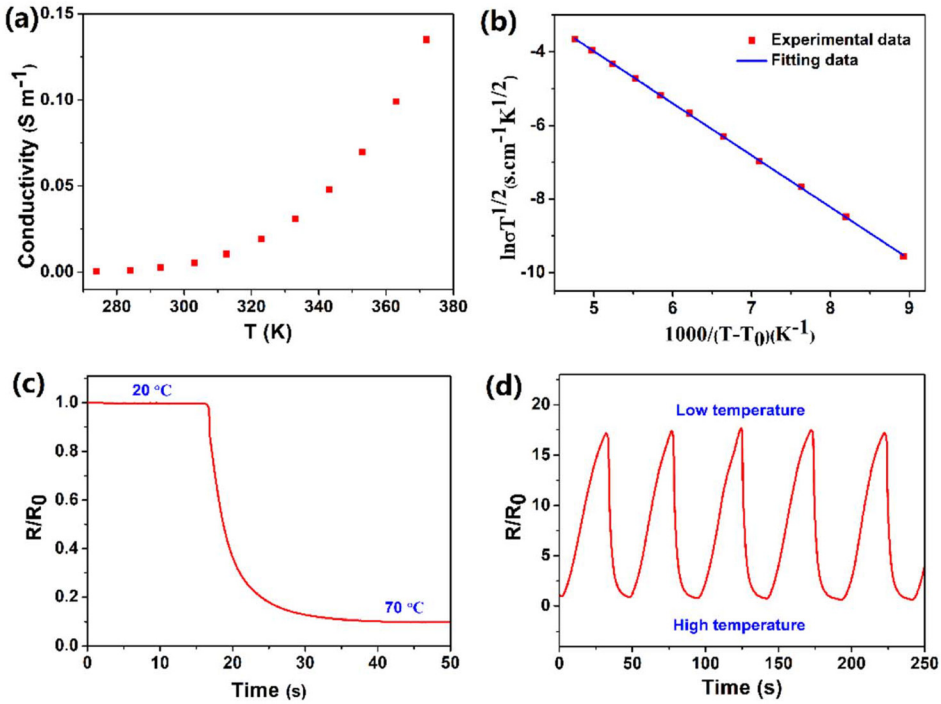

Fig. 4 (a) Temperature dependence of the conductivity of the PIL (from 273 K to 373 K). (b) VTF fitting curve of the conductivity of the PIL. (c) Time-dependent resistance evolution of the PIL for detecting temperature changes. (d) Time-dependent resistance evolution of the PIL for detecting regular temperature changes.

deformations. In contrast, ionic conductors generally have high stretchability but low sensitivity. As demonstrated in Fig. 3h, the PIL could monitor finger movement and distinguish between different finger angles, displaying its high stretchability. It is worth noting that owing to the high self-adhesion, the PIL could closely attach to the finger during the detection process, ensuring the accuracy of the detection. Besides probing large joint movements, the PIL also possessed high sensitivity to recognize tiny deformations, such as the human pulse (Fig. 3i). Therefore, the PIL can serve as a high-performance flexible strain sensor to monitor multiscale mechanical deformations.

It is the current trend and challenge to fabricate multimodal flexible sensors. For example, electronic skins which mimic human skin are usually required to detect temperature variation.[39,44] In this work, benefiting from its superior conductivity-temperature dependence, the PIL could be used as a high-performance temperature sensor. As illustrated in Fig. 4a, a rise in temperature improved the conductivity of the PIL, which is ascribed to the easier dissociation and mobility of ions at high temperatures. According to literature studies,[45] the relationship between the conductivity and temperature of PILs does not comply with the Arrhenius equation, but conforms to the VTF model:

$$\sigma T^{1/2} = A \exp\left(\frac{-B}{T-T_0}\right)$$

where A is the pre-exponential factor, B is the pseudo-activation energy, and T_0 is the thermodynamic glass-transition temperature of the ionogel at which the configuration entropy becomes zero. T_0 is usually about 20–50 K lower than the glass-transition temperature.[46,47] As illustrated in Fig. 4b, the experimental data of the PIL exhibited a perfect straight line and a high regression value of R^2 (reaches up to 0.999) emerged, demonstrating that the data fitted well to the VTF model. Therefore, the change in temperature of the PIL can be obtained by calculating the change in resistance through the VTF equation, which is the work mechanism of the PIL as a temperature sensor. Fig. 4c shows that increasing the temperature from 20 °C to 70 °C resulted in a rapid decrease of more than 90% in the resistance of the PIL, demonstrating the high response speed and excellent temperature detection sensitivity. Moreover, as depicted in Fig. 4d, the PIL temperature sensor exhibited superior stability and repeatability in detecting cyclic temperature changes. Therefore, the synthesized PIL could act as a high-performance temperature sensor with fast response speed, high sensitivity and superior repeatability, which can be used in many electronics, such as a heat-not-burn tobacco product, wearable human health monitoring equipment, and electronic skin.

4. Conclusion

In summary, in this study, by introducing a small amount of BA to copolymerize with [VBIM]TFSI, the mechanical properties of the PIL were greatly improved. The obtained PIL

exhibited high stretchability with strains exceeding 300% at the tensile strength of 75 kPa. Moreover, the obtained PIL possessed excellent environmental stability and superior self-adhesion. The outstanding electromechanical properties, such as high response speed, large stretchability, low hysteresis and remarkable repeatability, enable the PIL to serve as a high-performance flexible strain sensor to monitor different human activities, such as human joint movement and pulse. Furthermore, the PIL could be applied as a temperature sensor with high response speed, good sensitivity and superior repeatability. Therefore, this bimodal PIL flexible sensor presents great promise in flexible electronics.

Conflicts of interest

The authors declare no competing financial interest.

Acknowledgements

This work was supported by Natural Science Foundation of Gansu Province [grant number 21JR7RA091].

References

1 Y. Huang, X. Fan, S. C. Chen and N. Zhao, *Adv. Funct. Mater.*, 2019, **29**, 1808509.
2 H.-R. Lim, H. S. Kim, R. Qazi, Y.-T. Kwon, J.-W. Jeong and W.-H. Yeo, *Adv. Mater.*, 2020, **32**, 1901924.
3 S. Pyo, J. Lee, K. Bae, S. Sim and J. Kim, *Adv. Mater.*, 2021, **33**, 2005902.
4 Y. Chang, L. Wang, R. Li, Z. Zhang, Q. Wang, J. Yang, C. F. Guo and T. Pan, *Adv. Mater.*, 2021, **33**, 2003464.
5 W. A. D. M. Jayathilaka, K. Qi, Y. Qin, A. Chinnappan, W. Serrano-García, C. Baskar, H. Wang, J. He, S. Cui, S. W. Thomas and S. Ramakrishna, *Adv. Mater.*, 2019, **31**, 1805921.
6 C. Wang, K. Xia, H. Wang, X. Liang, Z. Yin and Y. Zhang, *Adv. Mater.*, 2019, **31**, 1801072.
7 S. Yao, P. Ren, R. Song, Y. Liu, Q. Huang, J. Dong, B. T. O'Connor and Y. Zhu, *Adv. Mater.*, 2019, **32**, 1902343.
8 M. J. Catenacci, C. Reyes, M. A. Cruz and B. J. Wiley, *ACS Nano*, 2018, **12**, 3689–3698.
9 C. Liu, S. Han, H. Xu, J. Wu and C. Liu, *ACS Appl. Mater. Interfaces*, 2018, **10**, 31716–31724.
10 J. Sun, Y. Yuan, G. Lu, T. Xue, J. Nie and Y. Lu, *Adv. Mater. Interfaces*, 2022, **9**, 2102245.
11 B. Yang and W. Yuan, *ACS Appl. Mater. Interfaces*, 2019, **11**, 16765–16775.
12 M. Wang, R. Li, X. Feng, C. Dang, F. Dai, X. Yin, M. He, D. Liu and H. Qi, *ACS Appl. Mater. Interfaces*, 2020, **12**, 27545–27554.
13 Y. Yuan, J. Zhou, G. Lu, J. Sun and L. Tang, *ACS Appl. Polym. Mater.*, 2021, **3**, 1610–1617.
14 H. Tang, J. Sun, X. Shu, Y. Zhao, J. Nie and X. Zhu, *ACS Appl. Polym. Mater.*, 2020, **2**, 4140–4148.
15 H. Zhang, W. Niu and S. Zhang, *ACS Appl. Mater. Interfaces*, 2018, **10**, 32640–32648.
16 J. Wu, Z. Wu, X. Lu, S. Han, B. R. Yang, X. Gui, K. Tao, J. Miao and C. Liu, *ACS Appl. Mater. Interfaces*, 2019, **11**, 9405–9414.
17 Q. Yang, Z. Zhang, X. G. Sun, Y. S. Hu, H. Xing and S. Dai, *Chem. Soc. Rev.*, 2018, **47**, 2020–2064.
18 Y. Kitazawa, K. Ueno and M. Watanabe, *Chem. Rec.*, 2018, **18**, 391–409.
19 J. Guo, Z. D. Tucker, Y. Wang, B. L. Ashfeld and T. Luo, *Nat. Commun.*, 2021, **12**, 437.
20 R. V. Barrulas, M. Zanatta, T. Casimiro and M. C. Corvo, *Chem. Eng. J.*, 2021, **411**, 128528.
21 S. G. Yoon, H. J. Koo and S. T. Chang, *ACS Appl. Mater. Interfaces*, 2015, **7**, 27562–27570.
22 D. Y. Choi, M. H. Kim, Y. S. Oh, S. H. Jung, J. H. Jung, H. J. Sung, H. W. Lee and H. M. Lee, *ACS Appl. Mater. Interfaces*, 2017, **9**, 1770–1780.
23 S. Chen, H. Liu, S. Liu, P. Wang, S. Zeng, L. Sun and L. Liu, *ACS Appl. Mater. Interfaces*, 2018, **10**, 4305–4314.
24 D. Mecerreyes, *Prog. Polym. Sci.*, 2011, **36**, 1629–1648.
25 W. Qian, J. Texter and F. Yan, *Chem. Soc. Rev.*, 2017, **46**, 1124–1159.
26 S.-Y. Zhang, Q. Zhuang, M. Zhang, H. Wang, Z. Gao, J.-K. Sun and J. Yuan, *Chem. Soc. Rev.*, 2020, **49**, 1726–1755.
27 J. Yuan and M. Antonietti, *Polymer*, 2011, **52**, 1469–1482.
28 A. S. Shaplov, R. Marcilla and D. Mecerreyes, *Electrochim. Acta*, 2015, **175**, 18–34.
29 H. Kokubo, R. Sano, K. Murai, S. Ishii and M. Watanabe, *Eur. Polym. J.*, 2018, **106**, 266–272.
30 A. Muñoz-Bonilla and M. Fernández-García, *Eur. Polym. J.*, 2018, **105**, 135–149.
31 S. Xiang, F. Zheng, S. Chen and Q. Lu, *ACS Appl. Mater. Interfaces*, 2021, **13**, 20653–20661.
32 J. Zhang, Z. Chen, Y. Zhang, S. Dong, Y. Chen and S. Zhang, *Adv. Mater.*, 2021, **33**, 2100962.
33 N. Sun, X. Gao, A. Wu, F. Lu and L. Zheng, *J. Mol. Liq.*, 2017, **248**, 759–766.
34 J. Sun, Y. Yuan, G. Lu, L. Li, X. Zhu and J. Nie, *J. Mater. Chem. C*, 2019, **7**, 11244–11250.
35 Y. Li, Z. Sun, L. Shi, S. Lu, Z. Sun, Y. Shi, H. Wu, Y. Zhang and S. Ding, *Chem. Eng. J.*, 2019, **375**, 121925.
36 X. Chen, S. Cao, W. Zhao and L. Chen, *J. Coat. Technol. Res.*, 2022, **19**, 887–895.
37 D. Zhou, R. Liu, J. Zhang, X. Qi, Y. B. He, B. Li, Q. H. Yang, Y. S. Hu and F. Kang, *Nano Energy*, 2017, **33**, 45–54.
38 S.-Y. Zhang, Q. Zhuang, M. Zhang, H. Wang, Z. Gao, J.-K. Sun and J. Yuan, *Chem. Soc. Rev.*, 2020, **49**, 1726–1755.
39 J. Sun, R. Li, G. Lu, Y. Yuan, X. Zhu and J. Nie, *J. Mater. Chem. C*, 2020, **8**, 8368–8373.
40 L. M. Zhang, Y. He, S. Cheng, H. Sheng, K. Dai, W. J. Zheng, M. X. Wang, Z. S. Chen, Y. M. Chen and Z. Suo, *Small*, 2019, **15**, e1804651.
41 S. Liu, R. Zheng, S. Chen, Y. Wu, H. Liu, P. Wang, Z. Deng and L. Liu, *J. Mater. Chem. C*, 2018, **6**, 4183–4190.

42 X. Tong, L. Du and Q. Xu, *J. Mater. Chem. A*, 2018, **6**, 3091–3099.
43 P. Yong-Lae, C. Bor-Rong and R. J. Wood, *IEEE Sens. J.*, 2012, **12**, 2711–2718.
44 C. Zhang, S. Song, Q. Li, J. Wang, Z. Liu, S. Zhang and Y. Zhang, *J. Mater. Chem. C*, 2021, **9**, 15337–15345.
45 F. Wu, N. Chen, R. Chen, Q. Zhu, J. Qian and L. Li, *Chem. Mater.*, 2016, **28**, 848–856.
46 F. Wu, N. Chen, R. Chen, Q. Zhu, G. Tan and L. Li, *Adv. Sci.*, 2016, **3**, 1500306.
47 J. Sun, G. Lu, J. Zhou, Y. Yuan, X. Zhu and J. Nie, *ACS Appl. Mater. Interfaces*, 2020, **12**, 14272–14279.